ORIGINAL ARTICLE

Protein profiling of conjunctival impression cytology samples of aniridia subjects

Tanja Stachon[1] ⓘ | Claudia Fecher-Trost[2] | Lorenz Latta[1] | Dalya Yapar[1] |
Fabian N. Fries[3] | Markus R. Meyer[2] | Barbara Käsmann-Kellner[3] | Berthold Seitz[3] |
Nóra Szentmáry[1]

[1]Dr. Rolf M. Schwiete Center for Limbal
Stem Cell and Aniridia Research,
Homburg/Saar, Germany

[2]Department of Experimental and Clinical
Toxicology, Institute of Experimental and
Clinical Pharmacology and Toxicology,
Center for Molecular Signaling (PZMS),
Saarland University, Homburg, Germany

[3]Department of Ophthalmology, Saarland
University Medical Center, Homburg/Saar,
Germany

Correspondence
Tanja Stachon, Dr. Rolf M. Schwiete
Center for Limbal Stem Cell and Aniridia
Research, Kirrberger Str. 100, Homburg/
Saar D-66424, Germany.
Email: tanja.stachon@uks.eu

Funding information
DOG Sektion Kornea, Grant/Award
Number: FF2021

Abstract

Purpose: Congenital aniridia is a rare disease, which is in most cases related to PAX6 haploinsufficiency. Aniridia associated keratopathy (AAK) also belongs to ocular signs of congenital aniridia. In AAK, there is corneal epithelial thinning, corneal inflammation, vascularization and scarring. In advanced stage AAK, typically, conjunctival epithelial cells slowly replace the corneal epithelium. Based on previous results we hypothesize that alterations of the conjunctival cells in congenital aniridia may also support the corneal conjunctivalization process. The aim of this study was to identify deregulated proteins in conjunctival impression cytology samples of congenital aniridia subjects.

Methods: Conjunctival impression cytology samples of eight patients with congenital aniridia [age 34.5 ± 9.9 (17–51) years, 50% female] and eight healthy subjects [age 34.1 ± 11.9 (15–54) years, 50% female] were collected and analysed using mass spectrometry. Proteomic profiles were analysed in terms of molecular functions, biological processes, cellular components and pathway enrichment using the protein annotation of the evolutionary relationship (PANTHER) classification system.

Results: In total, 3323 proteins could be verified and there were 127 deregulated proteins ($p < 0.01$) in congenital aniridia. From the 127 deregulated proteins (DEPs), 82 altered biological processes, 63 deregulated cellular components, 27 significantly altered molecular functions and 31 enriched signalling pathways were identified. Pathological alteration of the biological processes and molecular functions of retinol binding and retinoic acid biosynthesis, as well as lipid metabolism and apoptosis related pathways could be demonstrated.

Conclusions: Protein profile of conjunctival impression cytology samples of aniridia subjects identifies alterations of retinol binding, retinoic acid biosynthesis, lipid metabolism and apoptosis related pathways. Whether these changes are directly related to PAX6 haploinsufficiency, must be investigated in further studies. These new findings offer the possibility to identify potential new drug targets.

KEYWORDS
congenital aniridia, conjunctiva, proteomics

1 | INTRODUCTION

Congenital aniridia is a rare disease of the eye with an incidence of 1:100 000. It is a bilateral disease, which affects almost all eye structures (Hingorani et al., 2012). The ocular signs of congenital aniridia are aniridia associated keratopathy (AAK), secondary glaucoma, cataract, macular and optic nerve head hypoplasia (Ihnatko et al., 2013). In more than 90% of the cases, the cause of this panocular disease is PAX6 haploinsufficiency.

In AAK, there is corneal epithelial thinning, corneal inflammation, vascularization and scarring (Ihnatko

et al., 2013). So far, it has not been clarified whether the development of an AAK is a consequence of the progressive limbal stem cell insufficiency, or is rather related to other factors (Lagali et al., 2013; Latta, Figueiredo, et al., 2021; Latta, Knebel, et al., 2021; Latta, Ludwig, et al., 2021). Typically, conjunctival epithelial cells slowly replace the corneal epithelium, in advanced AAK stages (Puangsricharern & Tseng, 1995). One hypothesis is that the limbus is losing its natural ability to form a barrier between the conjunctiva and the cornea, which results in corneal conjunctivalization (Secker & Daniels, 2009). Nevertheless, based on results of our previous study, we also hypothesize that alterations of the conjunctival cells in congenital aniridia may also support the conjunctivalization process (Katiyar et al., 2021; Latta, Figueiredo, et al., 2021; Latta, Knebel, et al., 2021; Latta, Ludwig, et al., 2021).

As congenital aniridia is a rare disease, very often only a small amount of tissue or sample material is available for analysis. Nevertheless, it is important to examine as many different sample sources as possible and thus systematically investigate the causes of the disease.

Ihnatko et al. (2013) analysed protein expression in tear fluid of aniridia subjects by mass spectrometry and revealed an increased zinc-α2-glycoprotein and lactoferrin and a decreased α-enolase, peroxiredoxin 6, cystatin S, gelsolin and apolipoprotein A-1 protein level. Another study verified involvement of the conjunctiva is the disease process and described that these conjunctival changes deregulate numerous genes at mRNA level (Latta, Figueiredo, et al., 2021; Latta, Knebel, et al., 2021; Latta, Ludwig, et al., 2021). Latta et al. detected changes in miRNAs and transcripts regulating retinoic acid metabolism in conjunctival cells of aniridia subjects (Latta, Figueiredo, et al., 2021; Latta, Knebel, et al., 2021; Latta, Ludwig, et al., 2021). Based on these findings, it is known, that ocular surface changes in congenital aniridia are not only restricted to AAK, but there are also additional changes in the conjunctival epithelium. An additional important point is, that removal of conjunctival cells using impression cytology means no pain and nearly no risk for the patients, in contrast to potential difficulties regarding corneal impression cytology samples. However, this has not been further analysed at transcriptional level. Nevertheless, analysing the overlap of deregulated genes and proteins would allow us to draw conclusions about the pathogenesis of the disease and the related treatment options. It is of particular interest to know, which genes, proteins, and signalling pathways are affected in case of congenital aniridia.

Our purpose was to analyse protein expression in conjunctival cells of aniridia patients and healthy controls, using mass spectrometry.

2 | MATERIALS AND METHODS

2.1 | Patient and subject samples

This study was approved by the Ethics Committee of Saarland/Germany (No 110/17) and followed regulations of the Declaration of Helsinki. Informed written consent was obtained from all participants.

Eight aniridia subjects [age 34.5 ± 9.91 (17–51) years, 50% female] and eight healthy subjects [age 43.1 ± 11.9 (15–54) years, 50% female] have been recruited from the Department of Ophthalmology, Saarland University Medical Center, Homburg/Saar, Germany. Demographic data of all congenital aniridia and healthy subjects are displayed in Table 1. Conjunctival samples have been collected using EYEPRIM™ (Opia, Paris, France), from these 16 subjects. Thereafter, the samples were directly transferred into Lysis Buffer, provided by the DNA/RNA/Protein Purification Plus Micro Kit (Norgen Biotek Corp., Canada) and were stored at −80°C until RNA and protein extraction.

2.2 | Protein extraction

Proteins were extracted using the DNA/RNA/Protein Purification Plus Micro Kit (Norgen Biotek Corp.), according to the manufacturer's protocol.

2.3 | Protein measurement

For mass spectrometric analysis and Western Blot, protein quantity was determined as duplicate using Bradford assay, with bovine serum albumin as a standard. The measurements were performed following the manufactures' protocols (Sigma-Aldrich, Merck KGaA, Darmstadt, Germany). The absorbance was measured at 595 nm and the concentrations were quantified.

TABLE 1 Demographic data of aniridia and control subjects. The aniridia associated keratopathy (AAK) grading used classification of Lagali et al. (2020).

Subject number	Sex	Age	AAK grade right eye/left eye	Control	Sex	Age
AN2	M	42	2/3	Ctr1	F	32
AN4	M	51	5/4	Ctr3	F	29
AN6	F	35	4/4	Ctr5	M	27
AN8	F	33	No information	Ctr7	M	15
AN10	M	26	4/4	Ctr9	F	51
AN12	F	30	1/1	Ctr11	M	54
AN14	F	17	2/2	Ctr13	F	31
AN16	M	42	No information	Ctr15	M	34

2.4 | Mass spectrometric analysis of lysates of conjunctival cells from aniridia patients and control subjects

In this study, 20 µg of protein lysates were denatured for 20 min at 60°C in denaturing sample buffer (final concentration: 60 mM Tris HCl, pH 6.8, 4% SDS, 10% glycerol including 0.72 M β-mercaptoethanol). Lysates were shortly separated on NuPAGE® 4–12% gradient gels (ThermoFisher Scientific, Karlsruhe, Germany) until the bromophenol dye front migrated ~1.5 cm into the gel. After gel fixation (40% ethanol and 10% acetic acid) for 30 min proteins were visualized with colloidal Coomassie stain [20% (v/v) methanol, 10% (v/v) phosphoric acid, 10% (w/v) ammonium sulphate, and 0.12% (w/v) Coomassie G-250]. Four gel pieces were cut, washed, reduced, carbamidomethylated, and trypsin digested as described (Fecher-Trost et al., 2013). After extraction, 6 µL of tryptic peptides from each band were analysed by data-dependent nano-LC-ESI-HRMS/MS analysis. The setup contained an Ultimate 3000 RSLC nano LC equipped with an Ultimate 3000 RS autosampler coupled to a Thermo Scientific Orbitrap Eclipse Tribrid mass spectrometer (Thermo Scientific). Peptides were separated with a gradient generated with buffer A (0.1% formic acid) and buffer B (90% acetonitrile and 0.1% formic acid) at a flow rate of 300 nL/min: 0–5 min 4% B, 5–80 min to 31% B, 80–95 min to 50% B, 95–100 min to 90% B, 100–105 min hold 90% B, 105–106 min to 4% B and 106–120 min to 4% B. Tryptic peptides were trapped on a C18 trap column (75 µm × 2 cm, Acclaim PepMap100 C18, 3 µm), and separated on a reverse phase column (nano viper Acclaim PepMap capillary column, C18; 2 µm; 75 µm × 50 cm). The effluent was sprayed into the mass spectrometer using a coated emitter (PicoTipEmitter, 30 µm, New Objective, Woburn, MA, USA, ionization energy: 2.4 keV). MS^1 peptide spectra were acquired using the Orbitrap analyser ($R = 120$ k, RF lens = 30% m/z = 375–1500, MaxIT: auto, profile data, intensity threshold of 10^4). Dynamic exclusion of the 10 most abundant peptides was performed for 60 s. MS^2 spectra were collected in the linear ion trap (isolation mode: quadrupole, isolation window: 1.2, activation: HCD, HCD collision energy: 30%, scan rate: fast, data type: centroid).

2.5 | Raw data analysis of mass spectrometry results

Peptides and fragments were analysed using the TF PROTEOME DISCOVERER (PD) 1.4 software (ThermoFisher, Waltham, USA) using a MASCOT algorithm (Matrix Science). Briefly, peptides were matched to tandem mass spectra by MASCOT version 2.4.0 by searching of a SWISSPROT database (version 2021_05, number of protein sequences for all taxonomies: 564.638, for taxonomy human: 20.397). Peptides were analysed with the following mass tolerances: peptide tolerance: 10 ppm, fragment tolerance: 0.7 D. The PD workflow included tryptic digest and we allowed for up to two missed cleavage sites.

Cysteine carbamidomethylation was set as a fixed modification and deamidation of asparagine and glutamine, acetylation of lysine, and oxidation of methionine were set as variable modifications. The MASCOT output files (.dat) were loaded in the software SCAFFOLD (4.11.1, Proteome SoftwareInc., Portland, OR, USA) and spectra from the four separate gel bands belonging to one sample were combined with multidimensional protein-identification technology (MudPIT). Peptide identifications were accepted if those could be established at greater than 91.0% probability to achieve an FDR < 0.02% by the SCAFFOLD LOCAL FDR algorithm. Protein identifications were accepted if those could be established at greater than 98.0% probability to achieve an FDR < 4.4% and contained at least two identified peptides. Protein probabilities were calculated using the PROTEIN PROPHET algorithm (Nesvizhskii et al., 2003). Semi-quantitative analysis of the 16 patient samples was performed with SCAFFOLD based on spectral counting, using the same in the static and variable peptide modifications as in the PD search. One patient sample consists of four separate MS measurements, which were combined by multiplexing; altogether we made 64 MS sample runs for this study. Protein normalization was not applied to any values. For further analysis, the data were exported from SCAFFOLD to Excel.

2.6 | Bioinformatics

The gene ontology was analysed by the protein annotation of the evolutionary relationship (PANTHER) classification system (https://www.pantherdb.org) regarding molecular functions, cellular components, biological processes and reactome pathway enrichment analysis of deregulated proteins using the list of deregulated proteins with a *p*-value < 0.01, as input list. To demonstrate biological variances between samples, heat maps were created using MORPHEUS (http://software.broadinstitute.org/morpheus).

2.7 | Validation of deregulated proteins using Western blot

To validate protein expression, obtained from mass-spectrometry, PAX6, ADH7 and CRABP2 Western blot (WB) analysis has been performed, using 20 µg protein of the respective sample. The same samples have been used for mass-spectrometry and WB analysis.

PAX6 antibodies have been purchased from Sigma-Aldrich, ADH7 antibodies from Fisher Scientific (ThermoFisher Scientific™ GmbH, Dreieich, Germany) and CRABP2 from Abcam (Abcam, Berlin, Germany).

After boiling the samples for 5 min at 95°C, proteins were separated using NuPAGE™ bis-tris precast 4%–12% gels (ThermoFisher Scientific™ GmbH). Following protein separation, the proteins were transferred onto a nitrocellulose membrane with the Trans Blot Turbo Transfer System (BioRad, Hercules, CA, USA). Following blotting procedure, membranes were incubated with No-Stain™ Protein Labeling Reagent

(ThermoFisher Scientific™ GmbH). No-Stain™ Protein Labeling Reagent was used to visualize proteins on the membrane and to perform a total protein normalization, instead of a reference protein. Without additional destaining steps, primary antibodies were diluted in WesternFroxx anti-rabbit HRP solution, containing blocking reagent and secondary antibody (BioFroxx GmbH, Einhausen, Germany) and were added to the membrane, which was incubated overnight at 4°C. Visualization was performed using an imaging system (iBright, Thermo Fisher Scientific, Darmstadt, Germany). The IBRIGHT software performs densitometry on the No-Stain fluorescence of each lane's total protein and assigns a normalization factor of 1.0 of a chosen lane. The densitometric values of each lane were compared and each lane received an own normalization factor (Diller et al., 2021).

2.8 | Statistical analysis for Western blot evaluation

For statistical analysis, the GRAPHPAD PRISM 7.04 was used. Statistical analysis was performed using an unpaired t-test to compare both groups. p Values below 0.01 were considered statistically significant.

3 | RESULTS

3.1 | Proteomics data

Figure 1 summarizes our workflow and explains all the performed procedures more in detail.

We used a high-resolution mass spectrometric approach to investigate the protein expression profiles of conjunctival cells from control and aniridia patients. A total of 3323 human proteins were identified in both patient groups (Figure 2a; Table S1). In this study, 3142 proteins were detected in the conjunctival cells of aniridia patients, whereas 2438 proteins were identified in control patient samples (aniridia patients, $n=8$, control patients, $n=8$). Among the 3142 proteins identified in the aniridia patients, 885 were detected exclusively in this group, although equal amounts of protein were used as input and comparable numbers of MS spectra were measured within both sample groups. Table S1 displays a list of all detected proteins, a list of proteins exclusively detected in aniridia samples and a list of proteins exclusively detected in control samples. Using a cut off of $p<0.01$, 127 proteins were indicated as differentially abundant (Figure 2b). We next compared the semi-quantitative protein abundance of all proteins in the lysate by comparing the spectra counts of identified tryptic peptides
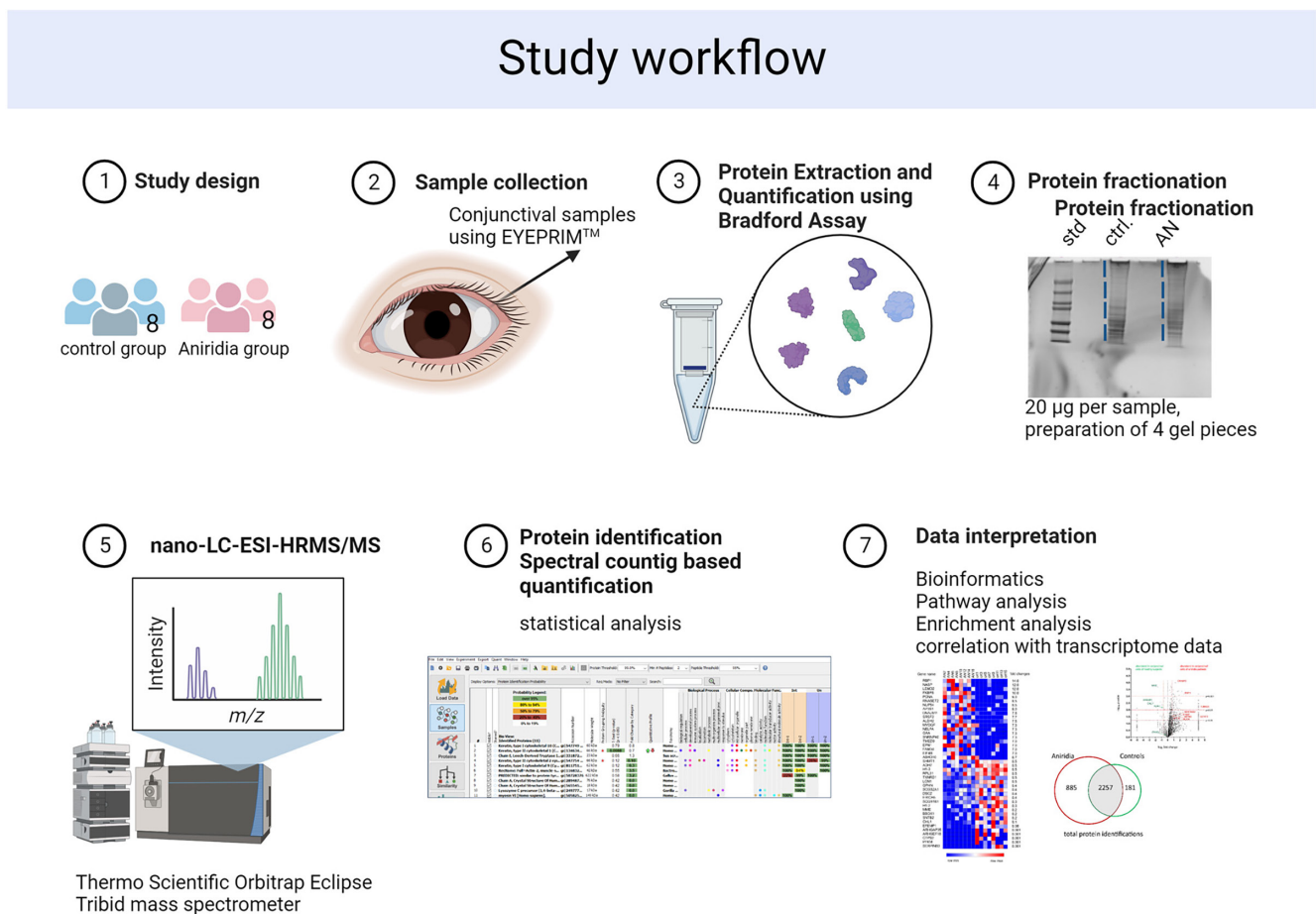

FIGURE 1 Scheme of nano-LC-ESI-HRMS/MS. Following sample collection, proteins were extracted, quantified and fractionated. After cleaning steps, samples were analysed by data-dependent nano-LC-ESI-HRMS/MS analysis. Peptides and fragments were analysed using the TF PROTEOME DISCOVERER (PD) 1.4 software using a MASCOT algorithm (Matrix Science). The MASCOT output files (.dat) were loaded in the software SCAFFOLD and SPECTRA from the four separate gel bands belonging to one sample were combined with multidimensional protein-identification technology (MudPIT). For further analysis, the data were exported from SCAFFOLD to Excel and heatmaps, pathway analysis, enrichment analysis were for data interpretation. (Created with BioRender.com).
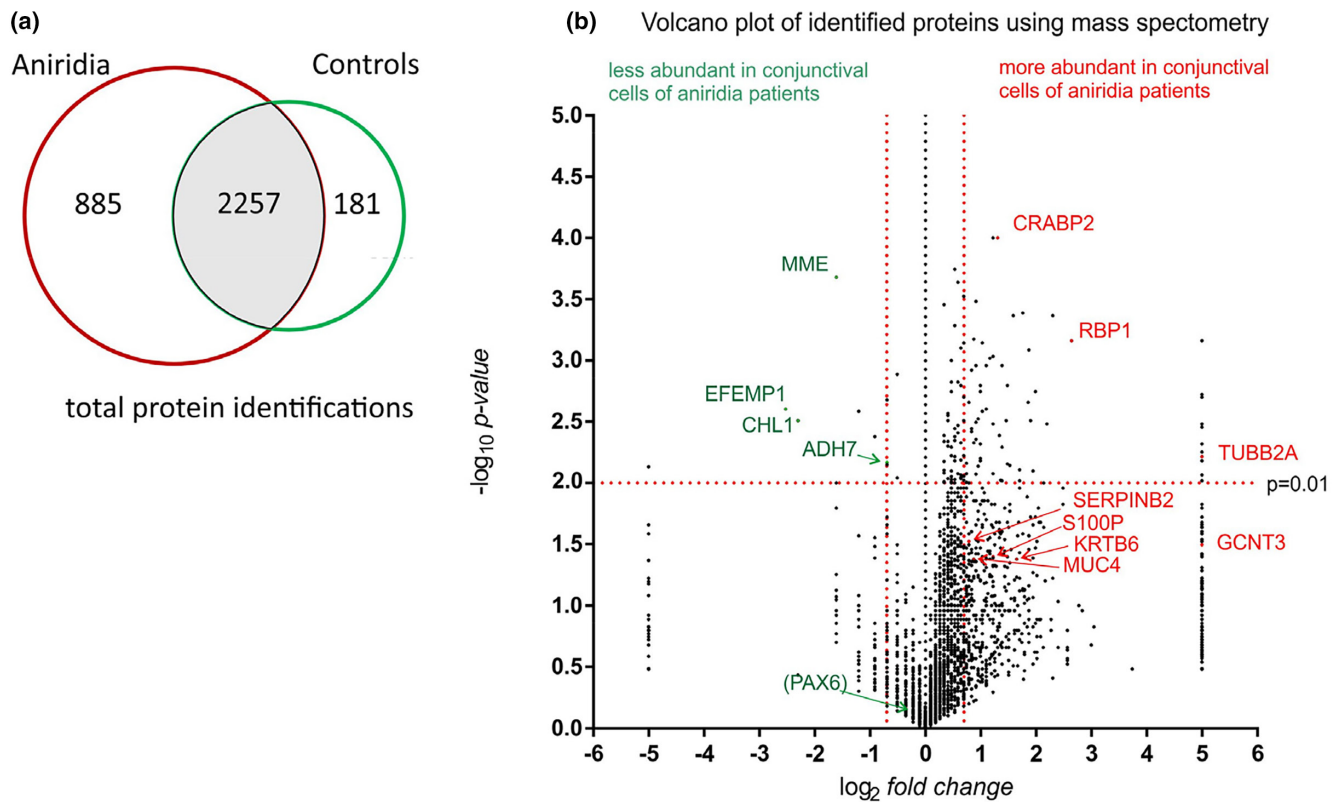
FIGURE 2 Proteins identified by nano-LC–MS/MS and differentially expressed proteins in aniridia and control conjunctival cells. The Venn diagram shows the number of MS identified proteins in protein lysate fractions from aniridia ($n=8$) and healthy control ($n=8$) subjects. Overall, 3142 proteins were analysed in the conjunctival cells of aniridia patients, whereas 2438 proteins were identified in control samples (a). The volcano plot of p-value versus $\log_2$-fold change (total spectra counts, semi-quantitative) summarizes the proteins differentially expressed in conjunctival cells of aniridia patients (b). Proteins are significantly (two-tailed Student's t-test, $p<0.01$) more abundant (upper-right) or less abundant (upper-left) in aniridia sample cells, in comparison to control cells. A complete list of proteins is summarized at Table S1.

(Figure 3). Total spectra of proteins identified by nano-LC-HR-MS/MS analysis are displayed from PAX6 and ADH7, CRABP2 and RBP1 as representative examples of deregulated proteins in Figure 3a–d.

Table S2 displays a list of all detected proteins, and a list of proteins belonging to different p-values.

Setting the final cut off for p-value <0.01, 127 proteins were used for enrichment analysis for biological processes, molecular function, cellular components and pathway analysis using the PANTHER classification system. From the 127 deregulated proteins (DEPs), 82 altered biological processes, 63 deregulated cellular components, 27 significantly altered molecular functions and 31 enriched signalling pathways were identified. The detailed list is shown at Table S3.

The valine catabolic process, the lipoprotein catabolic process, the branched-chain amino acid metabolic process, and the retinoic acid metabolic process have been identified between the 10 most deregulated biological processes (Figure 4a). For cellular components, the DEPs associated with aniridia were primarily enriched in mitochondrial complex and tricarboxylic acid (TCA) cycle enzyme complexes (Figure 4b). The most important molecular functions of the identified DEPs were porin activity, palmitoyl hydrolase activity and retinol binding (Figure 4c).

To provide insight into biological pathways associated with deregulated proteins identified in conjunctival cells of aniridia patients, reactome pathway analysis has been chosen, using the PANTHER classification system (version

17). The results indicated that apoptosome related pathways and pathways concerning amino acid catabolism were predominantly enriched (Figure 4d).

We have plotted the DEPs with a $p<0.01$ (127 proteins) in a heat map to demonstrate the distribution of up- and downregulated proteins in aniridia patients (Figure 5).

To determine whether the deregulated mRNAs from our previous study were also reflected in deregulated proteins of the current study, we performed an overlap analysis using VENNY (https://bioinfogp.cnb.es/tools/venny/index.html). For this analysis, for a better comparison to our previous study (Latta, Figueiredo, et al., 2021; Latta, Knebel, et al., 2021; Latta, Ludwig, et al., 2021), we set a cut off $p<0.05$ and FC<0.5 and >2 for both aniridia and control groups. We compared 511 deregulated mRNAs with 255 deregulated proteins. An overlap analysis of 511 deregulated mRNAs and 255 deregulated proteins revealed 12 overlaps (Table 2). In addition, in case of upregulated mRNAs, there were always upregulated proteins, and in case of downregulated mRNAs, there were always down-regulated proteins. Among these 12 overlaps were retinol-binding protein 1 (RBP1; FC$=14$, $p=0.00069$), cellular retinoic acid binding protein 2 (CRABP2; FC$=3.7$, $p<0.0001$) and aldehyde dehydrogenase 7 (ADH7; FC$=0.5$, $p=0.0068$).

Western blot analysis was done as an independent method for protein validation, to detect the expression of PAX6, ADH7 and CRABP2 in patient samples (see Figure S1). Western blot signals were obtained for ADH7 and PAX6, and densitometric analysis showed that
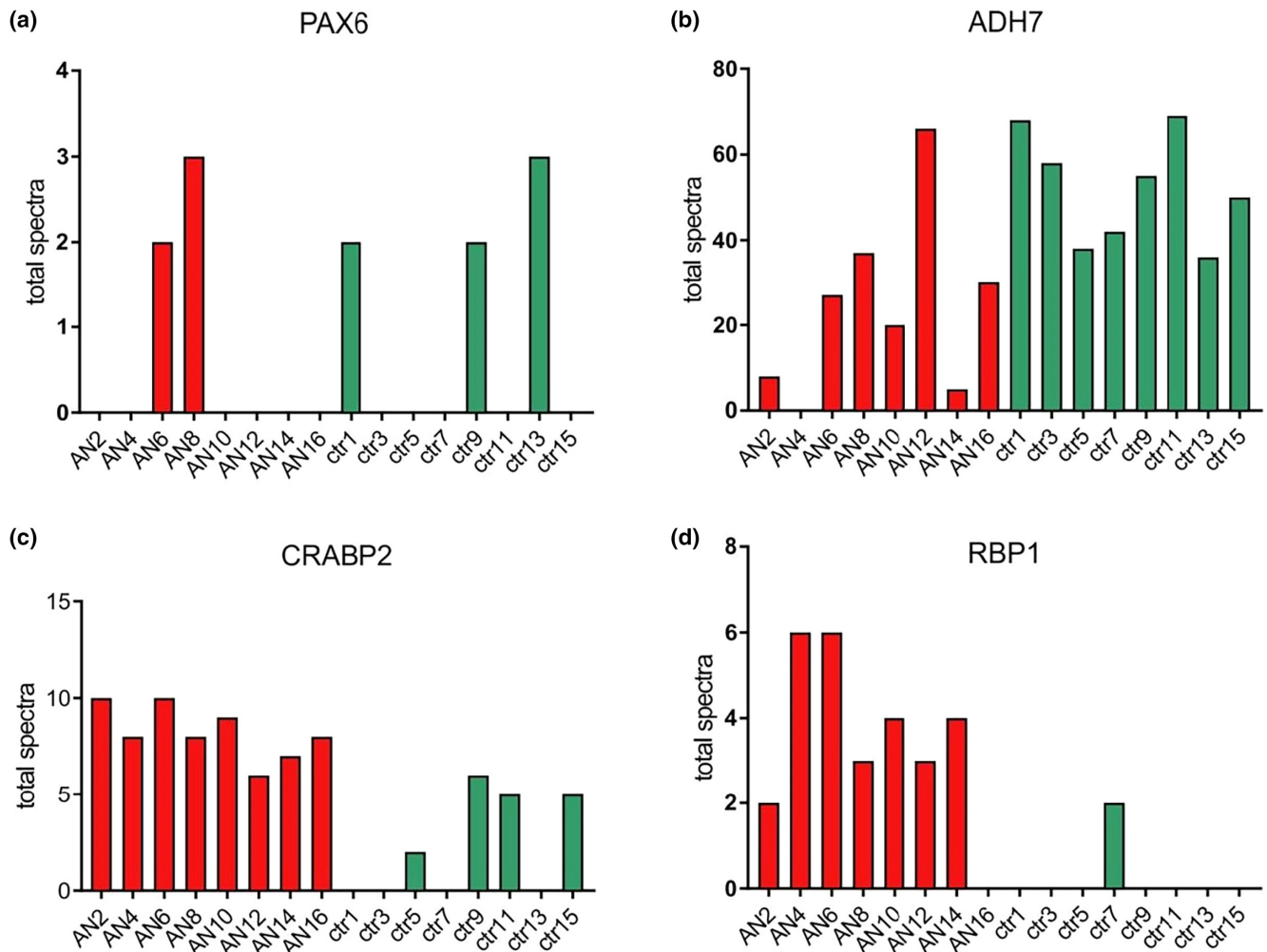
FIGURE 3 Comparison of individual protein expression levels in conjunctival cells of control and aniridia patients. The number of total tryptic spectra identified by nano-LC-HR-MS/MS analysis are displayed from PAX6 and ADH7, CRABP2 and RBP1 as representative examples of deregulated proteins (a–d).

expression levels did not differ between the two groups. CRAPBP2 protein was not detectable in conjunctival cell lysates by western blot analysis, whereas it was unambiguously identified by MS/MS analysis.

4 | DISCUSSION

The present study identified proteins from conjunctival impression cytology samples of aniridia subjects using high-resolution mass spectrometry (nano-LC-HR-MS/ MS). Protein analysis is a useful tool to identify potential treatment targets. Patient samples display more the real situation, than cell or animal models, which can only provide an approximation. Based on these data, we may be able to reveal the potential causative factors of AAK development and thus may be able to provide possible treatment options for patients with AAK. Since we know from our previous study, that there are also pathological changes of the conjunctival epithelium in aniridia patients, we aimed to analyse the proteome of conjunctival impression cytology samples of the same subjects, in the current study.

Impression cytology is a technique used for the evaluation of several ocular surface disorders like keratoconjunctivitis sicca, cicatricial pemphigoid, atopic diseases or limbal stem cell deficiency. It could be observed that in advanced AAK stages the corneal epithelium possesses a more conjunctival phenotype. Therefore, it may be difficult to differentiate between conjunctival and corneal epithelium.

The analysis of the current study resulted in the identification of a total of 3323 proteins and with a cut off p-value of <0.01, 127 proteins could be identified which are significantly deregulated in aniridia samples in comparison to controls. The identification of pathological alterations of the biological processes and molecular functions annotated in the Gene Ontology (GO), revealed alterations in lipoprotein catabolic processes, retinol binding functions, retinoic acid biosynthesis and defective intrinsic pathways for apoptosis for the 127 proteins, among others.

Under the 10 most deregulated biological processes analysed in the current study are protein depalmitoylation, branched-chain amino acid catabolism, and retinoic acid biosynthesis. Due to the increased catabolism of branched-chain amino acids in conjunctival cells of aniridia subjects, there could be alterations in fatty acid synthesis. Valine and leucine are in particular essential for this synthesis (Bishop et al., 2020) and lipids are necessary in order to recruit vesicle membranes during protein transportation from the endoplasmic reticulum to
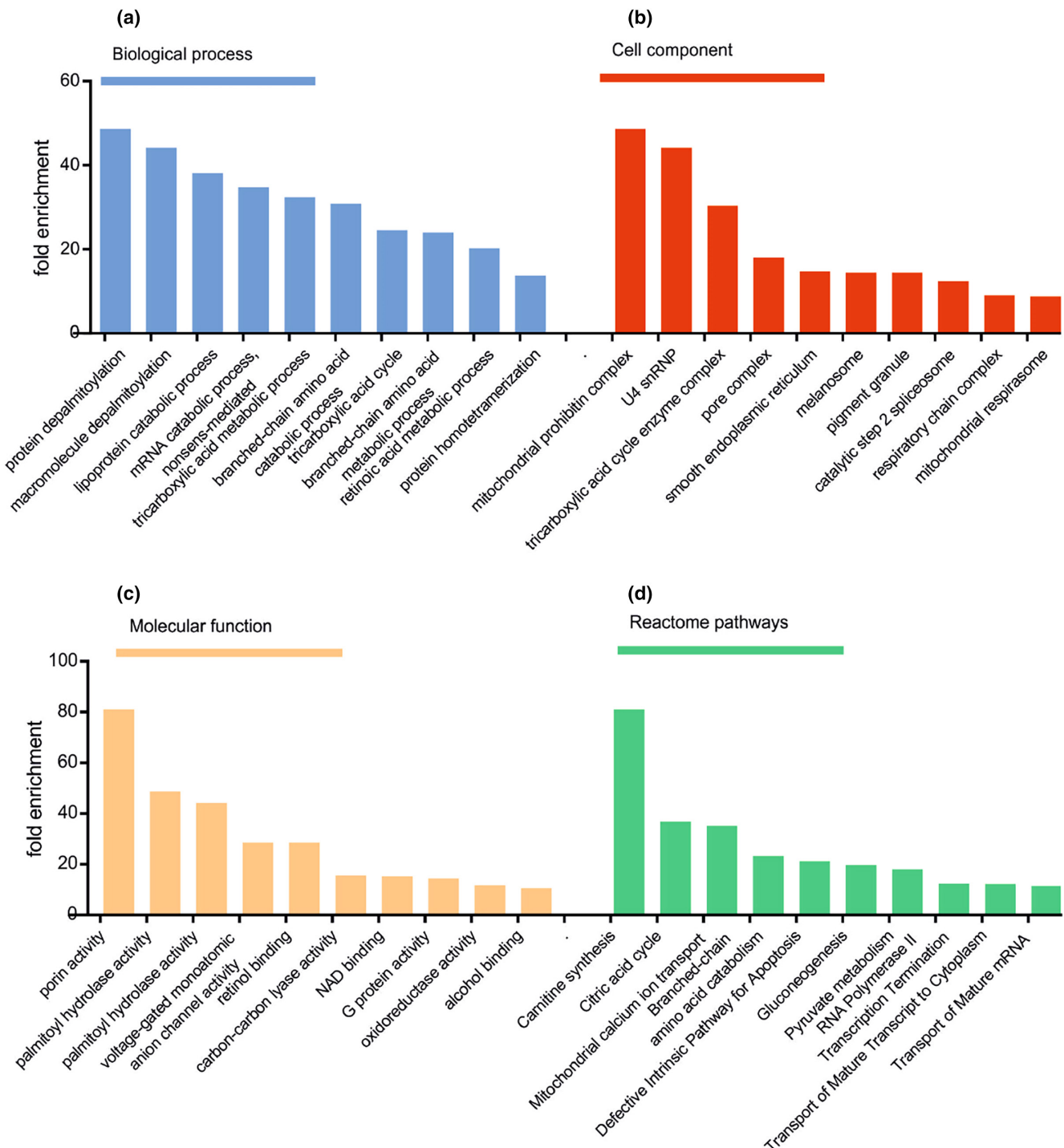
FIGURE 4 Profiling of the 10 most deregulated proteins (DEPs) in conjunctival epithelial cells of aniridia patients. The gene ontology categories of DEPs are (a) biological processes, (b) cellular components and (c) molecular functions. The 10 most enriched pathways are displayed in (d), using Reactome Pathway Database.

the Golgi apparatus. It is assumed that the composition of these lipids can regulate vesicle transport (Bonifacino & Glick, 2004). Cycles of depalmitoylation provide a mechanism for membrane sampling and trafficking of peripheral membrane proteins to the plasma membrane and are responsible for central regulators of cell growth and organization (Won et al., 2018).

Membrane lipids are constructed of fatty acids. These are required for cell and vesicle membranes, which transport proteins from the endoplasmic reticulum to the Golgi complex (Bonifacino & Glick, 2004). The Gene ontology of the DEPs of conjunctival epithelial cells of

aniridia patients indicated that some cell structures or cell components were altered in this disease. These include the mitochondrial prohibiting complex, and the tricarboxylic acid cycle (TCA cycle), which is directly related to various metabolic signalling pathways. The TCA cycle is a key metabolic pathway that connects carbohydrate, fat and protein metabolism (Martínez-Reyes & Chandel, 2020).

The reactome pathway enrichment analysis showed that under the 10 most enriched pathways the carnitine synthesis and the defective intrinsic pathway of apoptosis are altered. Carnitine is induced in antiapoptotic
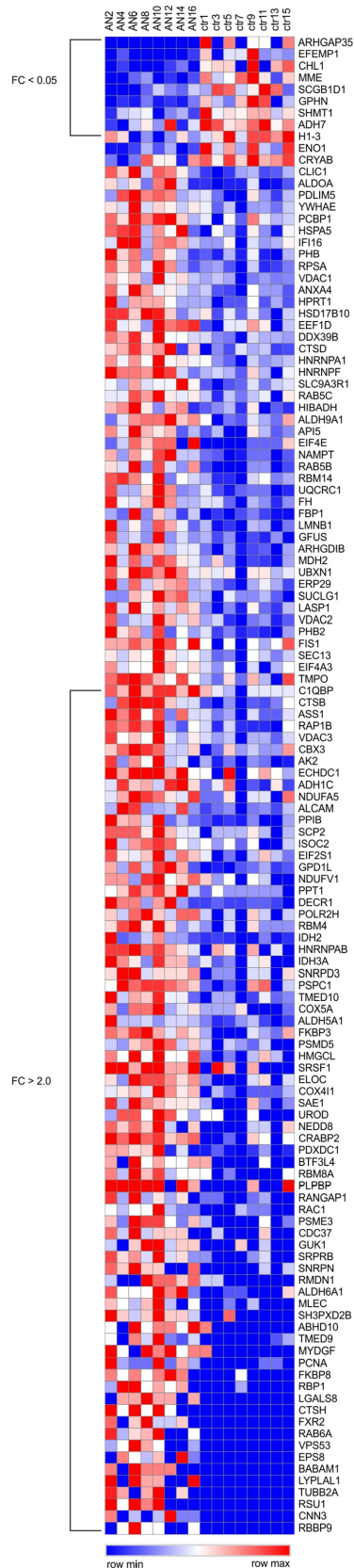
Column labels: AN2, AN4, AN6, AN8, AN10, AN12, AN14, AN16, ctr1, ctr3, ctr5, ctr7, ctr9, ctr11, ctr13, ctr15

FC < 0.05 group:
ARHGAP35, EFEMP1, CHL1, MME, SCGB1D1, GPHN, SHMT1, ADH7, H1-3, ENO1, CRYAB, CLIC1, ALDOA, PDLIM5, YWHAE, PCBP1, HSPA5, IFI16, PHB, RPSA, VDAC1, ANXA4, HPRT1, HSD17B10, EEF1D, DDX39B, CTSD, HNRNPA1, HNRNPF, SLC9A3R1, RAB5C, HIBADH, ALDH9A1, API5, EIF4E, NAMPT, RAB5B, RBM14, UQCRC1, FH, FBP1, LMNB1, GFUS, ARHGDIB, MDH2, UBXN1, ERP29, SUCLG1, LASP1, VDAC2, PHB2, FIS1, SEC13, EIF4A3, TMPO, C1QBP

FC > 2.0 group:
CTSB, ASS1, RAP1B, VDAC3, CBX3, AK2, ECHDC1, ADH1C, NDUFA5, ALCAM, PPIB, SCP2, ISOC2, EIF2S1, GPD1L, NDUFV1, PPT1, DECR1, POLR2H, RBM4, IDH2, HNRNPAB, IDH3A, SNRPD3, PSPC1, TMED10, COX5A, ALDH5A1, FKBP3, PSMD5, HMGCL, SRSF1, ELOC, COX4I1, SAE1, UROD, NEDD8, CRABP2, PDXDC1, BTF3L4, RBM8A, PLPBP, RANGAP1, RAC1, PSME3, CDC37, GUK1, SRPRB, SNRPN, RMDN1, ALDH6A1, MLEC, SH3PXD2B, ABHD10, TMED9, MYDGF, PCNA, FKBP8, RBP1, LGALS8, CTSH, FXR2, RAB6A, VPS53, EPS8, BABAM1, LYPLAL1, TUBB2A, RSU1, CNN3, RBBP9

row min — row max

FIGURE 5 Heatmap reporting semi-quantitative analysis of proteins identified by mass spectrometry in conjunctival cell lysates of control and aniridia patients. The *Z*-scores of total spectral counts (PSM) summarized from eight individual samples/group (AN=aniridia, ctr=control) are shown. Deregulated proteins with a *p*-value <0.01were used for analysis. Rows are identified by Entrez gene names. Intensities are shown by a colour range, from red (row max) to white (row average) and to blue (row minimum). The graphic was assessed by the software MORPHEUS (http://software.broadinsti tute.org/morpheus).

processes like inhibition of oxidative stress induced apoptosis in corneal epithelial cells (Khandekar et al., 2013). It is known that aniridia epithelial cells show an increased apoptosis rate (Calvão-Pires et al., 2014). Ihnatko et al. (2013) assumed that in corneal epithelial cells of aniridia patients the increased oxidative stress resulted in increased apoptosis and abnormal wound healing (Ihnatko et al., 2013). If several signalling pathways are altered, this certainly leads to increased cell stress and thus to an increased apoptosis rate. In PAX6$^{+/-}$ mice, corneas showed higher rates of apoptotic stromal cells compared to wild-type mice (Ramaesh et al., 2006). We may summarize that in conjunctival cells of aniridia patients the apoptotic processes are also activated.

Using the criteria $p < 0.01$ and FC <0.5|>2, our study revealed that the most upregulated protein is retinol binding Protein 1 (RBP1; FC=14.0).

RPB1 binds to retinol and prevents retinoids from being non-specifically oxidized. RPB1 then transports the retinoids for further synthesis into retinoic acid (Yu et al., 2022). In PAX6$^{-/-}$ mice *RBP1* was found to be expressed at low levels (Holm et al., 2007). Interestingly, in our current study, we demonstrate the opposite expression in PAX6 haploinsufficient aniridia patients. This may happen due to the counter-regulation of the remaining PAX6 gene, nevertheless the question remains, why an increased RBP1 expression is required. To answer this question, further research needs to be conducted.

Under down-regulated proteins the Rho GTPase-activating protein35 (ARHGAP35) (FC=0.001), neprilysin (MME; FC=0.2), and all-trans-retinol dehydrogenase 7 (ADH7; FC=0.5) have been verified.

ARHGAP35 is fundamental in eye development and responsible for ocular disorders like microphthalmia and anophthalmia (Reis et al., 2023). It plays a role in cell migration, invasion and division and can directly regulate the cytoskeleton reorganization. A decreased ARHGAP35 level is correlated with a decreased E-cadherin level, which is associated with a decreased cell survival (Sun et al., 2022). Neprilysin, or MME, is a membrane metallo-endopeptidase and its expression is elevated in kidney biopsies of patients with chronic kidney disease, which is associated with kidney fibrosis. Inhibition of neprilysin can lead to reduced levels of inflammation related markers like TNF-α, IL-1β and IL-6 (Lai et al., 2023). As mentioned before, ADH7 is reduced in aniridia limbal epithelial cells and contributes to retinol oxidation. The enzyme encoded by the *ADH7* gene is most active as a retinol dehydrogenase; thus, it may participate in the synthesis of retinoic acid, which is important for cellular differentiation, which has been shown to be pathologically altered in aniridia corneal epithelial cells and affected by PAX6 (Collinson et al., 2004).

Patients with congenital aniridia almost all develop AAK in the course of the disease. AAK severity correlates with degradation of palisade structures and therefore, with limbal stem cell deficiency (Lagali et al., 2013). Analysing our congenital aniridia samples, we could identify valine catabolic process, the lipoprotein catabolic process, the branched-chain amino acid metabolic process, and the retinoic acid metabolic process, between the 10 most deregulated biological processes,

TABLE 2 Comparison of deregulated mRNAs and proteins detected in conjunctival samples of aniridia subjects.

Protein name	Entrez identifier	mRNAs identified by mRNA-array (Latta, Ludwig, et al., 2021)	Proteins identified by nano-LC-HR-MS/MS (current study)
ADH7	P40394	↓	↓
CHL1	O00533	↓	↓
MME	P08473	↓	↓
EFEMP1	Q12805	↓	↓
S100P	P25815	↑	↑
TUBB2A	Q13885	↑	↑
SERPINB2	P05120	↑	↑
CRABP2	P29373	↑	↑
GCNT3	O95395	↑	↑
KRT6B	P04259	↑	↑
RBP1	P09455	↑	↑
MUC4	Q99102	↑	↑

Note: There were 12 overlapping mRNA/protein identifiers after analysing 511 deregulated mRNAs from an earlier study Latta, Ludwig, et al. (2021) and 255 proteins from the current study (criteria: $p<0.05$ and FC$<0.5|>2$).

which may also be related to limbal stem cell deficiency. Nevertheless, these biological processes, and their correlation with limbal stem cell deficiency needs more detailed analysis in the future. In congenital aniridia subjects, there is also dry eye disease, with impaired corneal epithelial cell differentiation and impaired wound healing of the corneal surface (Yazdanpanah et al., 2020). Progressive AAK is accompanied by a decrease of visual acuity, in AAK Stage 4 with a vascularized corneal scar, including the optical axis (Ihnatko et al., 2016).

So far, there is no standardized treatment of AAK. This can be explained by the fact that congenital aniridia is a rare disease, making it difficult to establish treatment guidelines. In addition, the exact causes of the development of an AAK cannot be precisely defined either, yet. Therefore, it would be of utmost importance to identify the trigger, resulting in differentiation disorder of the corneal epithelium. The amount of PAX6 protein in aniridia patient corneal epithelial cells with PAX6 haploinsufficiency is usually 60%–70% of those in healthy subjects (Leiper et al., 2006). At the same time, keratin 12 protein expression, which is considered as a marker for corneal epithelial cell differentiation, is lacking in aniridia corneal epithelial cells (Dua et al., 2003). Nevertheless, other signalling pathways like Notch, Wnt and TGF-β signalling pathways, which also have a role in cell differentiation, may also be affected by the persistently reduced PAX6 protein supply (Li et al., 2015). Zhang et al. showed that in mouse embryonic stem cells, *PAX6* mRNA expression increased after retinoic acid administration and could trigger cell differentiation (Okada et al., 2004) (Wu et al., 2016). This may also be an explanation for the insufficient differentiation of corneal epithelial cells of congenital aniridia subjects. Of course, PAX6 deficiency due to haploinsufficiency and an additional disturbance of retinoic acid metabolism could result in a severe disturbance of corneal epithelial cell differentiation. Most interestingly, aniridia associated keratopathy has also been treated by topical all-trans retinoic acid (ATRA) in some cases (Tan et al., 2016).

A further interesting finding is the difference in keratin expression of aniridia and control conjunctival samples. There were six keratins, which were exclusively expressed in aniridia-samples: KRT6C, KRT20, KRT23, KRT31, KRT85 and KRT86, whereas KRT74 was only detected in control samples. The keratinization is a typical phenomenon in AAK and can be observed at microscopic examination (Lee et al., 2008). Nevertheless, KRT3 and KRT12, which are regulated by PAX6, were expressed in the aniridia and the control groups, without a significant difference.

Our previous findings described pathological expression of several mRNAs in the transcriptome of conjunctival epithelial cells of aniridia subjects. Therefore, we planned to evaluate the proteome of conjunctival epithelial cells of aniridia patients, as well.

The conjunctival goblet cells (CGCs) are conjunctival cells producing soluble mucins like MUC5AC. Their lower density can result in corneal keratinization and opacity, which phenomenon is also observed in aniridia subjects. The number of goblet cells is negatively correlated with the progression of conjunctival inflammation (Swamhynathan & Wells, 2020). Nevertheless, with higher AAK grades, the density of inflammatory cells also increases (Lagali et al., 2013). Although MUC5AC protein expression of conjunctival cells of our studied aniridia patients was slightly increased compared to controls, this did not reach statistical significance. Therefore, at least using this method, we cannot prove a change of goblet cell density in AAK subjects.

It is worth to notice that 885 proteins, are exclusively detected in aniridia samples, using a cut-off of $p<0.01$. Tubulin beta-2A chain is the protein with the most spectra and relates to cellular proliferation, movement and adhesion (Shin et al., 2020). Interestingly, tubulin beta-2A was also upregulated at transcriptional level in our previous study (Latta, Ludwig, et al., 2021). Therefore, tubulin beta-2A function also needs further clarification in congenital aniridia.

The group of Soria analysed conjunctival cells from patients with dry eye and meibomian gland dysfunction using 2D-DIGE (Soria et al., 2018). The proteome of tears in aniridia patients was observed by Ihnatko et al. (2013). Nevertheless, to the best of our knowledge, there is no previous study that has examined the proteome of conjunctival cells from aniridia patients, using mass spectrometry. Our data provide a useful basis for further research in finding therapeutic targets, which could reduce cell stress in aniridia subjects, thus facilitating treatment in AAK and slowing down its pathogenesis.

4.1 | Limitation of the study

Epithelial cell samples were collected from the conjunctiva of aniridia patients, for the present study. Therefore, unfortunately, no direct correlations regarding conjunctival and corneal epithelial changes can be drawn from the present data.

5 | CONCLUSIONS

In summary, conjunctival epithelial cells of aniridia patients show alterations in retinol and lipid metabolism and an increased propensity to apoptosis at protein level. The collected data provide an important basis for further studies to understand the pathomechanism and to find possible treatment targets in AAK.

ORCID
Tanja Stachon https://orcid.org/0000-0001-7009-7125

REFERENCES
Bishop, C.A., Schulze, M.B., Klaus, S. & Weitkunat, K. (2020) The branched-chain amino acids valine and leucine have differential effects on hepatic lipid metabolism. *The FASEB Journal*, 34, 9727–9739.

Bonifacino, J.S. & Glick, B.S. (2004) The mechanisms of vesicle budding and fusion. *Cell*, 116, 153–166.

Calvão-Pires, P., Santos-Silva, R., Falcão-Reis, F. & Rocha-Sousa, A. (2014) Congenital Aniridia: clinic, genetics, therapeutics, and prognosis. *International Scholarly Research Notices*, 2014, 305350.

Collinson, J.M., Chanas, S.A., Hill, R.E. & West, J.D. (2004) Corneal development, limbal stem cell function, and corneal epithelial cell migration in the Pax6+/− mouse. *Investigative Ophthalmology and Visual Science*, 45, 1101–1108.

Diller, T., Thompson, J. & Steer, B. (2021) Biological validation of a novel process and product for quantitating western blots. *Journal of Biotechnology*, 326, 52–60.

Dua, H.S., Joseph, A., Shanmuganathan, V.A. & Jones, R.E. (2003) Stem cell differentiation and the effects of deficiency. *Eye*, 17, 877–885.

Fecher-Trost, C., Wissenbach, U., Beck, A., Schalkowsky, P., Stoerger, C., Doerr, J. et al. (2013) The in vivo TRPV6 protein starts at a non-AUG triplet, decoded as methionine, upstream of canonical initiation at AUG. *Journal of Biological Chemistry*, 288, 16629–16644.

Hingorani, M., Hanson, I. & Van Heyningen, V. (2012) Aniridia. *European Journal of Human Genetics*, 20, 1011–1017.

Holm, P.C., Mader, M.T., Haubst, N., Wizenmann, A., Sigvardsson, M. & Götz, M. (2007) Loss- and gain-of-function analyses reveal targets of Pax6 in the developing mouse telencephalon. *Molecular and Cellular Neurosciences*, 34, 99–119.

Ihnatko, R., Eden, U., Fagerholm, P. & Lagali, N. (2016) Congenital Aniridia and the ocular surface. *The Ocular Surface*, 14, 196–206.

Ihnatko, R., Edén, U., Lagali, N., Dellby, A. & Fagerholm, P. (2013) Analysis of protein composition and protein expression in the tear fluid of patients with congenital aniridia. *Journal of Proteomics*, 94, 78–88.

Katiyar, P., Stachon, T., Fries, F.N., Parow, F., Ulrich, M., Langenbucher, A. et al. (2021) Decreased FABP5 and DSG1 protein expression following PAX6 knockdown of differentiated human limbal epithelial cells. *Experimental Eye Research*, 215, 108904.

Khandekar, N., Willcox, M.D.P., Shih, S., Simmons, P., Vehige, J. & Garrett, Q. (2013) Decrease in hyperosmotic stress-induced corneal epithelial cell apoptosis by L-carnitine. *Molecular Vision*, 19, 1945–1956.

Lagali, N., Edén, U., Utheim, T.P., Chen, X., Riise, R., Dellby, A. et al. (2013) In vivo morphology of the limbal palisades of vogt correlates with progressive stem cell deficiency in aniridia-related keratopathy. *Investigative Ophthalmology and Visual Science*, 54, 5333–5342.

Lagali, N., Wowra, B., Fries, F.N., Latta, L., Moslemani, K., Utheim, T.P. et al. (2020) Early phenotypic features of aniridia-associated keratopathy and association with PAX6 coding mutations. *The Ocular Surface*, 18, 130–140.

Lai, W., Huang, R., Wang, B., Shi, M., Guo, F., Li, L. et al. (2023) Novel aspect of neprilysin in kidney fibrosis via ACSL4-mediated ferroptosis of tubular epithelial cells. *MedComm*, 4, e330.

Latta, L., Figueiredo, F.C., Ashery-Padan, R., Collinson, J.M., Daniels, J., Ferrari, S. et al. (2021) Pathophysiology of aniridia-associated keratopathy: developmental aspects and unanswered questions. *The Ocular Surface*, 22, 245–266.

Latta, L., Knebel, I., Bleil, C., Stachon, T., Katiyar, P., Zussy, C. et al. (2021) Similarities in DSG1 and KRT3 downregulation through retinoic acid treatment and PAX6 knockdown related expression profiles: does PAX6 affect RA signaling in Limbal epithelial cells? *Biomolecules*, 11, 1651.

Latta, L., Ludwig, N., Krammes, L., Stachon, T., Fries, F.N., Mukwaya, A. et al. (2021) Abnormal neovascular and proliferative conjunctival phenotype in limbal stem cell deficiency is associated with altered microRNA and gene expression modulated by PAX6 mutational status in congenital aniridia. *The Ocular Surface*, 19, 115–127.

Lee, H., Khan, R. & O'Keefe, M. (2008) Aniridia: current pathology and management. *Acta Ophthalmologica*, 86, 708–715.

Leiper, L.J., Walczysko, P., Kucerova, R., Ou, J., Shanley, L.J., Lawson, D. et al. (2006) The roles of calcium signaling and ERK1/2 phosphorylation in a Pax6+/− mouse model of epithelial wound-healing delay. *BMC Biology*, 4, 27.

Li, G., Xu, F., Zhu, J., Krawczyk, M., Zhang, Y., Yuan, J. et al. (2015) Transcription factor PAX6 (paired box 6) controls limbal stem cell lineage in development and disease. *The Journal of Biological Chemistry*, 290, 20448–20454.

Martínez-Reyes, I. & Chandel, N.S. (2020) Mitochondrial TCA cycle metabolites control physiology and disease. *Nature Communications*, 11, 102.

Nesvizhskii, A.I., Keller, A., Kolker, E. & Aebersold, R. (2003) A statistical model for identifying proteins by tandem mass spectrometry. *Analytical Chemistry*, 75, 4646–4658.

Okada, Y., Shimazaki, T., Sobue, G. & Okano, H. (2004) Retinoic-acid-concentration-dependent acquisition of neural cell identity during in vitro differentiation of mouse embryonic stem cells. *Developmental Biology*, 275, 124–142.

Puangsricharern, V. & Tseng, S.C.G. (1995) Cytologlogic evidence of corneal diseases with Limbal stem cell deficiency. *Ophthalmology*, 102, 1476–1485.

Ramaesh, T., Ramaesh, K., Leask, R., Springbett, A., Riley, S.C., Dhillon, B. et al. (2006) Increased apoptosis and abnormal wound-healing responses in the heterozygous Pax6+/− mouse cornea. *Investigative Ophthalmology and Visual Science*, 47, 1911–1917.

Reis, L.M., Chassaing, N., Bardakjian, T., Thompson, S., Schneider, A. & Semina, E.V. (2023) ARHGAP35 is a novel factor disrupted in human developmental eye phenotypes. *European Journal of Human Genetics*, 31, 363–367.

Secker, G.A. & Daniels, J.T. (2009) Limbal epithelial stem cells of the cornea. In: *StemBook [Internet]*. Cambridge, MA: Harvard Stem Cell Institute. Available from: https://doi.org/10.3824/stembook.1.48.1

Shin, D., Park, J., Han, D., Moon, J.H., Ryu, H.S. & Kim, Y. (2020) Identification of TUBB2A by quantitative proteomic analysis as a novel biomarker for the prediction of distant metastatic breast cancer. *Clinical Proteomics*, 17, 1–19.

Soria, J., Acera, A., Durán, J.A., Boto-de-Los-Bueis, A., Del-Hierro-Zarzuelo, A., González, N. et al. (2018) The analysis of human conjunctival epithelium proteome in ocular surface diseases using impression cytology and 2D-DIGE. *Experimental Eye Research*, 167, 31–43.

Sun, Y., Du, R., Shang, Y., Liu, C., Zheng, L., Sun, R. et al. (2022) Rho GTPase-activating protein 35 suppresses gastric cancer metastasis by regulating cytoskeleton reorganization and epithelial-to-mesenchymal transition. *Bioengineered*, 13, 14605–14615.

Swamhynathan, S. & Wells, A. (2020) Conjunctival goblet cells:ocular surface functions, disorders that affect them, and the potential for their regeneration. *The Ocular Surface*, 18, 19–26.

Tan, J.C.K., Tat, L.T. & Coroneo, M.T. (2016) Treatment of partial limbal stem cell deficiency with topical interferon α-2b and retinoic acid. *The British Journal of Ophthalmology*, 100, 944–948.

Won, S.J., Cheung See Kit, M. & Martin, B.R. (2018) Protein depalmitoylases. *Critical Reviews in Biochemistry and Molecular Biology*, 53, 83–98.

Wu, C.-Y., Persaud, S.D. & Ei, L.-N. (2016) Retinoic acid induces ubiquitination-resistant RIP140/LSD1 complex to fine-tune PAX6 gene in neuronal differentiation. *Stem Cells*, 34, 114–123.

Yazdanpanah, G., Bohm, K.J., Hassan, O.M., Karas, F.I., Elhusseiny, A.M., Nonpassopon, M. et al. (2020) Management of Congenital Aniridia-Associated Keratopathy: long-term outcomes from a tertiary referral center. *American Journal of Ophthalmology*, 210, 8–18.

Yu, J., Perri, M., Jones, J.W., Pierzchalski, K., Ceaicovscaia, N., Cione, E. et al. (2022) Altered RBP1 gene expression impacts epithelial cell retinoic acid, proliferation, and microenvironment. *Cell*, 11, 792.

SUPPORTING INFORMATION

Additional supporting information can be found online in the Supporting Information section at the end of this article.

How to cite this article: Stachon, T., Fecher-Trost, C., Latta, L., Yapar, D., Fries, F.N., Meyer, M.R. et al. (2024) Protein profiling of conjunctival impression cytology samples of aniridia subjects. *Acta Ophthalmologica*, 102, e635–e645. Available from: https://doi.org/10.1111/aos.16614